Direct Dimethyl Ether Polymer Electrolyte Fuel Cells for Portable Applications

M. M. Mench,*,z H. M. Chance, and C. Y. Wang*

*Electrochemical Engine Center and Department of Mechanical and Nuclear Engineering,
The Pennsylvania State University, University Park, Pennsylvania 16802, USA*

Dimethyl ether (DME) is a potential fuel for direct oxidation fuel cells that combines the main advantages of hydrogen (pumpless fuel delivery) and methanol (high energy density storage). DME also has low toxicity compared to methanol, making it a potential fuel for portable applications. This paper describes performance aspects and limitations of the DME fuel cell. At the anode, there is a critical balance between water and DME availability for reaction that suggests a thin electrolyte to promote back diffusion of water to the anode is desirable for high performance. However, excessive DME or DME intermediate crossover reaction losses with a Pt/Ru anode and Pt cathode catalyst preclude use of the thinnest electrolytes available.
© 2003 The Electrochemical Society. [DOI: 10.1149/1.1631819] All rights reserved.

Due to safety and technical barriers associated with the use of hydrogen or methanol as fuel, significant effort has gone into searching for an alternative to the hydrogen polymer electrolyte fuel cell (H$_2$ PEFC) or direct methanol fuel cell (DMFC) for portable power.[1-13] A detailed review of H$_2$ PEFCs or DMFCs is not within the scope of this paper; the reader is referred to reviews on H$_2$ and DMFCs by Gottesfeld and Lamy *et al.*, respectively.[14,15]

Due to molecular simplicity and ease of oxidation, H$_2$ PEFCs have a high power density (~0.7 W/cm^2). However, hydrogen suffers from low storage density and lack of storage, generation, and distribution infrastructure. The DMFC has been developed for portable applications because the system requires less ancillary equipment and is therefore more simplified compared to an H$_2$ PEFC. Reduced performance of the DMFC compared to the H$_2$ PEFC is deemed tolerable in light of the ease and storage density of liquid fuel. However, for portable applications, the DMFC has major disadvantages in terms of fuel storage density and toxicity.[16] Low anode methanol concentrations of 0.5-2 M are typically needed to prevent excessive fuel crossover losses.[17-20] This level of dilution requires an undesirable amount of water carried with the fuel flow. Even at the theoretical maximum methanol molarity of 16.8 M (one mole of water is needed per mole of methanol for the anodic oxidation reaction), there is a significant amount of water storage that needs to be considered in system power density calculations. In terms of toxicity, methanol is poisonous if imbibed orally or inhaled in large quantities, spreads rapidly into ground water, has a colorless flame, and is more corrosive than gasoline.

Dimethyl ether.—Dimethyl ether (DME) is the simplest ether expressed by the chemical formula, CH$_3$OCH$_3$. DME is a colorless, chemically stable liquid and gas, with bp −25.1°C at atmospheric pressure. It is typically stored as a liquid at 0.6 MPa (75 psig) in standard propane tanks. DME is presently used as an aerosol and propellant for spray paints, agricultural chemicals, and cosmetics, and is a potential diesel fuel replacement.[21,22] Benefits of the use of DME for fuel cells include:

1. High electron transfer number of 12 for complete oxidation (methanol is 6 and hydrogen is 2) resulting in reduced theoretical fuel requirement.

2. Lack of C—C bond makes complete direct electro-oxidation possible with minimal kinetic losses, compared to other more complex compounds.[5]

3. Reduced expected crossover rate due to reduced dipole moment of DME compared to methanol.

4. Potential storage as a high density liquid at 0.6 MPa (75 psig). This pressure can be used to drive fuel flow for a pumpless portable

DME system. In this sense, fuel delivery would be similar to a butane lighter, with liquid storage at high pressure and delivery as a gas phase at low pressure.

5. The low toxicity of DME is comparable to that of liquid propane.[23] Comparatively, methanol is toxic upon skin contact and ingestion.

6. Handling properties are similar to those of propane and butanes; therefore, existing liquid propane infrastructure and handling technologies can be used to store and transport DME.

7. DME will not spread into groundwater as does methanol.

8. DME has a higher autoignition temperature and lower flammability limit than gasoline.[23]

9. The DME lower explosion limit is higher than that of propane, and DME has a visible flame. In comparison, hydrogen and methanol flames are nearly invisible.

10. DME decomposes in atmosphere in several tens of hours; therefore, DME is not a greenhouse gas, nor does it degrade the ozone layer.[24]

DMEFC.—So far, very little characterization of the DMEFC has taken place. Table I presents some basic thermochemical parameters of DME and other typical fuels for comparison. Müller and co-workers examined DME fuel cell performance and fuel utilization compared to the DMFC at high pressure (5 atm) and temperature (130°C), and found performance similar to DMFC under these operating conditions.[5] They utilized a 49 cm^2 active area Nafion 117 electrolyte with a Pt/Ru anode and Pt black cathode, both with catalyst loadings of 4 mg/cm^2. The high pressure and temperature studied, however, are not suited for portable applications. Based on cyclic voltammography and gas chromatography results, Müller also concluded that DME crossover from the anode to cathode does not react at the cathode, leading to reduced cathode losses compared to DMFC. Tsutsumi and co-workers have also studied the DMEFC and shown substantial performance enhancement for elevated temperature (100-130°C) and pressure (4.5 atm).[25,26] They showed that injection of up to 4% DME into the oxygen cathode stream of a H$_2$ fuel cell (FC) resulted in minimal performance degradation. Interestingly, DME has also been proposed for use in solid oxide[27] and molten carbonate[28] fuel cells. The motivation for this paper was to examine the limitations and performance of the DMEFC at less extreme conditions of pressure and temperature than tested by Müller and coworkers or Tsutsumi and co-workers in order to determine DMEFC suitability.

Experimental

Both a 5 cm^2 and a 50 cm^2 active area FC were used in this study. The flow fields for the reactants were a serpentine-parallel combination. A schematic of the test and control system is shown in Fig. 1. The test system is designed to easily switch between liquid methanol solution and gas-phase fuel flow. DME and standard dry air were supplied from compressed gas-cylinders. Liquid methanol

* Electrochemical Society Active Member.
z E-mail: mmm124@psu.edu

Table I. Basic thermochemical parameters of DME and other typical fuels.

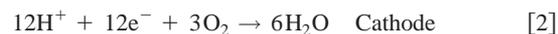| Property	DME CH$_3$OCH$_3$	Methanol CH$_3$OH	Hydrogen H$_2$	Propane C$_3$H$_8$	Diesel fuel (low sulfur mix)
Boiling point, °C	−24.8	64.7	−252.8	−42	180-370
Liquid density, 20°C (g/cm^3)	0.67	0.79	NA	0.49	0.83-0.86
Gas specific gravity relative to air at 1 atm	1.59	NA	0.07	1.52	>1.0
Autoignition temperature (°C)	235	464	565.5	450	257
Flammability limit (%) range	3.4-27	6.0-36	4.0-74.2	2.1-9.5	0.6-7.5
NFPA hazard rating (Health/flammability/reactivity)	2/4/1	1/3/0	0/4/0	1/4/0	0/2/0

solution was delivered from a reservoir pressurized with nitrogen. Bubble-type humidifiers were used to provide desired humidification to anode and cathode flows when needed. Between humidifier and FC, electric heating tapes were installed to maintain desired temperature conditions and prevent condensation of humidified flow. All reactant inputs to the fuel cell, and the FC itself, were main-

Figure 1. Schematic of the experimental test stand and control system used in this study.

tained at the desired temperature with several Omega Engineering, Inc. model 8500 PID controllers. To control and measure accurate current/voltage polarization data, the fuel cell was interfaced to a potentiostat/galvanostat system from Arbin Instruments, Inc. It should be noted that the stoichiometries reported here are at a chosen current density. That is, flowrate was kept constant over the entire polarization curve and was not varied with current. Thus, flow rate is reported as an equivalent maximum current density.

The membrane electrode assemblies (MEAs) used in this study were manufactured by Lynntech Inc. (College Station, Texas). Each MEA had a 4 mg/cm^2 Pt/Ru unsupported anode catalyst loading with a 1:1 Pt/Ru atomic ratio and a 4 mg/cm^2 unsupported Pt cathode loading. Catalysts used by Lynntech Inc. for MEA construction were manufactured by Alfa Aesar. Nafion 117, 115, and 112 were used as the electrolyte, and a single-sided Elat (De Nora N.A., Inc. E-Tek Division) gas diffusion layers were used.

Results and Discussion

DME operational requirements.—Anode water and DME stoichiometry.—Like hydrogen, DME is a gas at room temperature and pressure. Like methanol, DME consumes water as part of the anodic oxidation reaction. However, DME requires three times the moles of water for oxidation compared to methanol, which can lead to significant anode drying. Since DME has limited solubility in water (1.65 M at STP), it cannot be delivered at ambient pressure in high concentration to the anode in solution, and the anode gas must be humidified to achieve proper performance.[23] DME undergoes the following global anode oxidation and cathode reduction reactions

$$(CH_3)_2O + 3H_2O \rightarrow 2CO_2 + 12H^+ + 12e^- \quad \text{Anode} \quad [1]$$

$$12H^+ + 12e^- + 3O_2 \rightarrow 6H_2O \quad \text{Cathode} \quad [2]$$

The anode DME stoichiometry can therefore be shown as

$$\xi_{DME} = \frac{12F\dot{n}_{DME}}{iA_{Rx}} \quad [3]$$

where i is the current density and A_{Rx} is the superficial electrode area. Because water is also a reactant, we can define a water anode stoichiometry as well

$$\xi_{H2O} = \frac{4F\dot{n}_{H2O}}{iA_{Rx}} \quad [4]$$

Considering an anode DME and water vapor flow mixture, the water stoichiometry is related to the DME stoichiometry through thermodynamics of psychrometric mixtures
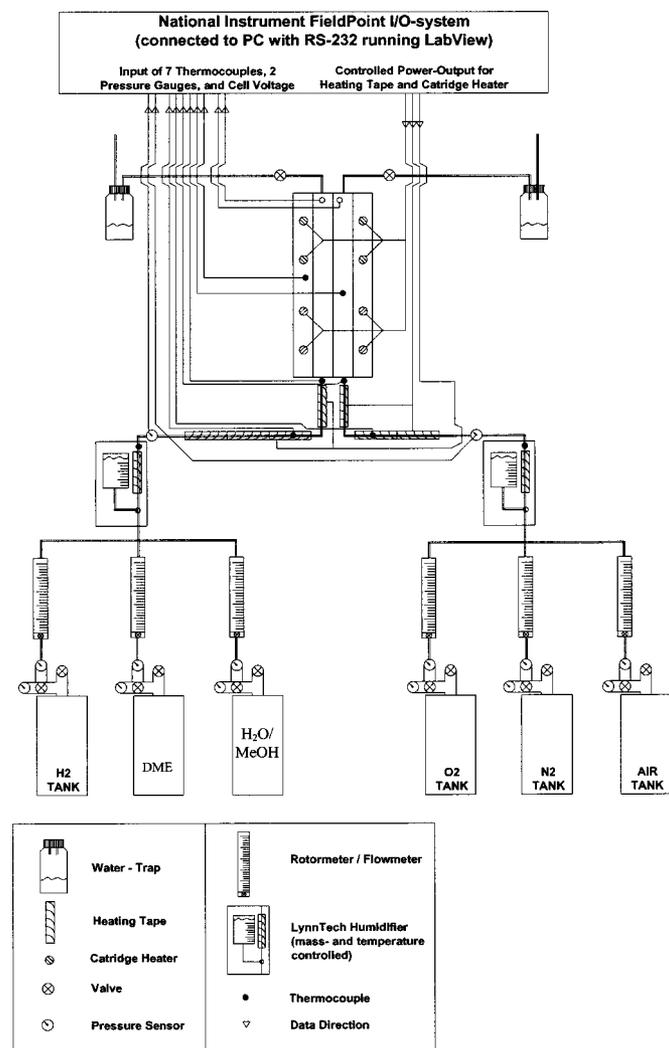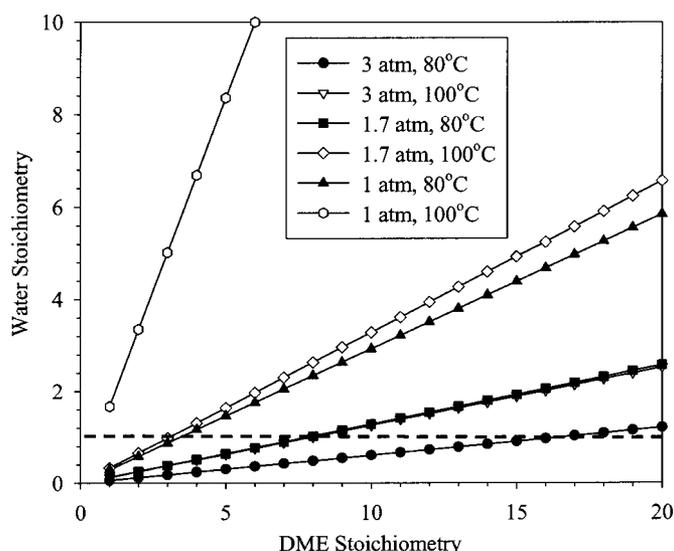
Figure 2. Plot of DME fuel cell inlet stoichiometry *vs.* fuel cell inlet water stoichiometry as a function of operating pressure and temperature, assuming fully humidified anode inlet flow. A dashed line is shown for water stoichiometry of unity.

$$\xi_{H2O} = \frac{\dot{n}_{H2O,del}}{\dot{n}_{H2O,req}} = \frac{\xi_{dme}\left(\dfrac{1}{P_{t,a}/P_{sat}RH - 1}\right)\dfrac{iA_{Rx}}{12F}}{\dfrac{iA_{Rx}}{4F}}$$

$$= \frac{\xi_{dme}\left(\dfrac{1}{P_{t,a}/P_{sat}RH - 1}\right)}{3} \qquad [5]$$

where RH is the relative humidity of the anode gas mixture, $P_{t,a}$ is the anode inlet total pressure, and P_{sat} is the thermodynamic saturation pressure of the mixture, a highly nonlinear function of temperature. A plot of the relationship between DME and water stoichiometry is shown in Fig. 2. Temperature and pressure have a strong effect. At low pressure, the water stoichiometry is more favorable due to higher saturated water mole fraction. Higher temperatures also allow greater saturation pressure of water, thus requiring a lower minimum DME stoichiometry to provide adequate moisture for fuel.

From another perspective, based on the anode oxidation reaction for DME shown in Eq. 1, the required molar flow ratio of water to DME is 3 to 1, assuming zero net flux of water from anode to cathode. This ratio provides just enough water to assist the oxidation reaction. Additional water may be needed to overcome the combined effect of back diffusion and electro-osmotic drag, if the net flux is toward the cathode. A plot showing the critical threshold for a 3:1 ratio as a function of anode temperature and pressure is shown in Fig. 3. Typically, thin membranes such as Nafion 112 (51 μm thickness) have near zero net water flux while thicker membranes such as Nafion 117 (178 μm) have a positive net flux of water toward the cathode for H_2 PEFC.[29] Clearly, unless a net flow of water from the cathode to anode can be achieved, high temperatures with full humidification and low operating pressure are needed to achieve adequate moisture content.

Two major points concerning the results of these figures should be made. Note that both Fig. 2 and Fig. 3 assume the sole source of water is from the anode inlet in vapor form, where more or less water may be required to overcome the net effect of electro-osmotic drag and back diffusion. Second, the calculations do not indicate the effect of mass transport limitation to the anode catalyst layer. Even
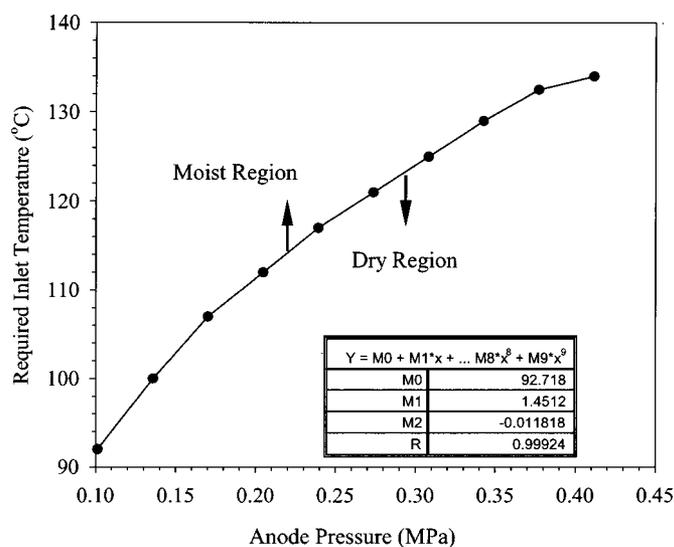

Figure 3. Relationship between anode pressure and fully humidified anode inlet temperature to satisfy required 3:1 molar ratio for electrochemical reaction. This assumes no net drag of water from anode to cathode and all water is supplied to the anode by fully humidified vapor-phase water. Above the curve, there is adequate water for reaction, below the curve, there will not be adequate water for electrochemical oxidation of DME.

though a high temperature low-pressure system is ideal from a water transport perspective, the resulting low bulk DME mole fraction can result in transport limitations from the gas channel to the catalyst layer.

Anode water starvation by electro-osmotic drag and the critical nature of back diffusion.—Here, the possibility of a dry anode resulting from electro-osmotic drag from the anode to cathode is examined. A polymer electrolyte membrane (PEM) that is less than fully saturated has poor conductivity, thus greatly reducing performance. DME stoichiometry can be written as

$$\xi_{DME} = \frac{c_{DME}\nu A_x}{\dfrac{i_{ref}A_{Rx}}{12F}} \qquad [6]$$

where, ν = gas mixture inlet velocity, i_{ref} is the reference current density on which the stoichiometry is defined, F is the Faraday constant, and A_x is the gas channel cross-sectional area. To prevent anode dryout at the fuel cell exit, it can be shown (see Appendix for derivation) that the flow stoichiometry must satisfy the following condition

$$\xi_{DME}i_{ref} \geq 12i(n_d + 0.25)\left(\frac{P}{P_{sat}RH} - 1\right) \qquad [7]$$

where n_d is the electro-osmotic drag coefficient. Considering $i_{ref} = i$, then we yield a current-independent result

$$\xi_{DME,crit} \geq 12(n_d + 0.25)\left[\frac{P}{P_{sat}RH} - 1\right] \qquad [8]$$

Note that we have assumed zero back diffusion, which from this result will be shown to be critical. As a sample calculation, assuming n_d is ~1.0-2.5 based on literature,[30,31] P is 200,000 Pa, P_{sat} is 47,000 Pa (for 80°C), inlet RH is 100%, and $i = i_{ref}$

$$\xi_{DME} \geq (15\text{-}33)\left[\frac{2}{0.47} - 1\right] = (48.8\text{-}106.4) = 48.8\text{-}106.4 \quad [9]$$

Therefore, in the absence of back diffusion, the anode side will be effectively dried from electro-osmotic drag, unless a DME stoichiometry of 50-100 is provided, which is unreasonable. Note that this multiplier of 50-100 compares to one of only 1.2-2 for a H_2 cell. However, the DME multiplier drops to ~28 for 90°C operation (~5 at atmospheric pressure), and zero for temperatures > 100°C.

This calculation illustrates that back diffusion is an important mode of water transport for the DMEFC. Thus, the DMEFC has a balance between DME and water mole fraction. Anode humidification, low pressure, high temperature, and high back diffusion (via thin MEA) are all critical.

Influence of membrane preconditioning procedure on performance.—It is known that membrane performance for DMFC is enhanced by performing certain preconditioning procedures in a hydrogen/air environment. Testing of several membranes demonstrated that the DMEFC had nearly zero performance if the MEA was initially preconditioned in a humidified hydrogen/air environment. However, stable DMEFC performance resulted if the MEA was first preconditioned using a methanol solution. Performance enhancement attributed to methanol preconditioning was also observed in formic acid FC.[32] In that study, the authors attributed the increased performance on pore alignment in the anode catalyst layer during preconditioning in methanol, or CO_2 bubbles from methanol oxidation increasing porosity in the cast Nafion film. Pore alignment could be responsible for the preconditioning effect seen for the DMEFC, but it is unknown why methanol would have a greater enhancement than hydrogen. In the case of DMEFC, the performance enhancement could be a result of interaction with surface adsorption of CO by methanol reaction intermediates. Because it is known that catalyst-bound CO is a critical step in the methanol oxidation process,[8,33,34] it is expected that operation on methanol will produce a catalyst surface at least partially covered in adsorbed CO, despite the bimetallic addition of Ru catalyst.

To verify if the adsorbed CO plays a critical role in membrane preconditioning, a hydrogen mixture with 50 ppm CO contaminant was used to precondition a new MEA. Results indicated that preconditioning the membrane with hydrogen doped with 50 ppm CO was nearly as effective in pretreating the membrane for DME operation as methanol. It should be noted that after preconditioning, the DMEFC could be operated in a stable manner for several hours with no degradation in performance. This indicates that the adsorbed CO was not consumed by the reaction without replacement, but somehow enabled the DME oxidation process to occur.

Performance with Nafion 117 electrolyte.—For a series of tests, Nafion 117 electrolyte was used. Figure 4 shows three DMEFC polarization and power density curves taken for an initial solution of DME dissolved in water at room temperature (Approximately 1.65 M solution), with nonhumidified cathode airflow. It is important to note that although the data in Fig. 4 were obtained with an initial solution of DME dissolved in water at room temperature, pure vapor DME was fed to a humidifier for all other data presented in this paper. Note the low relative performance for the case of unheated direct liquid DME dissolved in solution. Since DME is not completely miscible in water, a liquid solution of DME and water suffers severe fuel mass transport limitations. That is, as the liquid solution is heated above ambient temperature upon entering the fuel cell, it releases DME in vapor phase, leaving the liquid solution in contact with the anode DME depleted. In this condition, the anode was essentially flooded. For the gas-phase fuel-feed cases shown in Fig. 4, the initial 1.65 M fuel solution was heated to boiling point and vaporized before entering the FC. Very little difference was observed in performance for increased cathode pressure from 1.7 to 3 atm. Note that for all three curves, a sharp mass limiting cut-off was observed.

In order to determine the relative roles of ohmic resistance, anode kinetics, and mass transport, the cathode flow was replaced with oxygen and a polarization curve taken in air and oxygen is shown in Fig. 5. The lack of enhanced performance with oxygen replacement
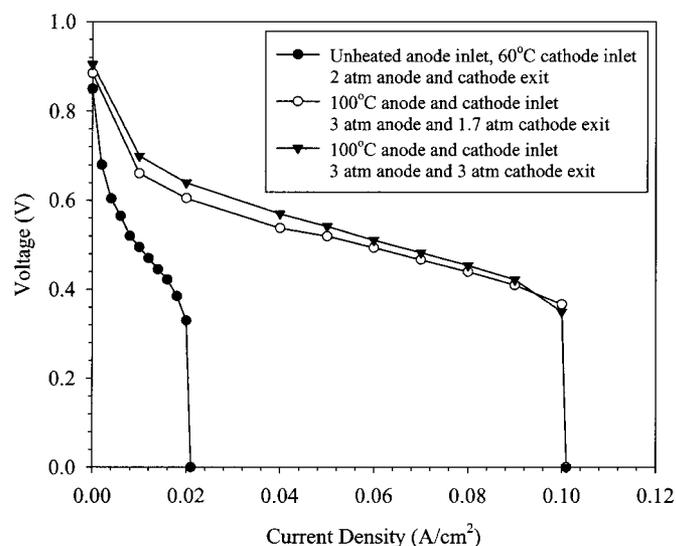

Figure 4. Polarization curves as a function of temperature and cathode pressure. Nafion 117 electrolyte. Common conditions: unhumidified cathode, ξ_{DME}: 1.875 A/cm² equivalent (constant flow rate), ξ_c: 1.875 A/cm² equivalent (constant flow rate).

indicates a great majority of losses occur as ohmic or anode activation losses for this arrangement with Nafion 117 electrolyte.

Performance results with Nafion 115 electrolyte.—As shown in the section on DME operational requirements, there is a critical need for water at the anode side for the electrochemical oxidation reaction. However, excessive humidification of the anode fuel flow stream can also result in high dilution and subsequent DME starvation. It is thus critical to provide adequate water to the anode by back-diffusion through the electrolyte. Because this mode of water transport is enhanced by a thinner electrolyte, Nafion 115 (127 µm thick) was used to compare to results with the Nafion 117 (187 µm thick) electrolyte. Figures 4 and 5 show that operation of a DMEFC with a Nafion 117 electrolyte resulted in a sharp mass limited drop-
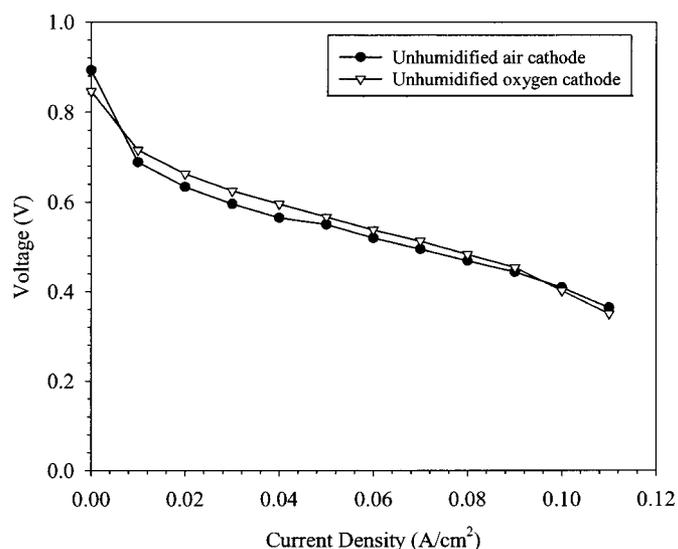

Figure 5. DME polarization curves as a function of cathode oxygen mole fraction. Nafion 117 electrolyte. Test conditions: cell temperature: 100°C, fully humidified DME anode, unhumidified air cathode, anode/cathode pressure: 3/1.7 atm, ξ_{DME}: 1.875 A/cm² equivalent (constant flow rate), ξ_c: 1.875 A/cm² equivalent (constant flow rate).
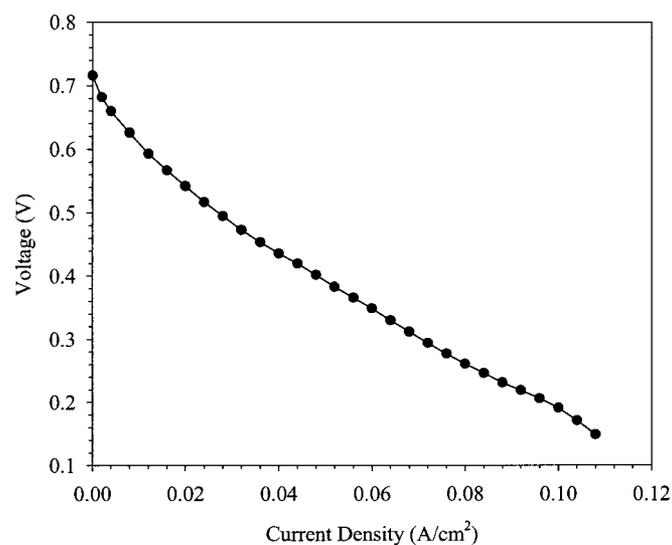
Figure 6. DME polarization curve with Nafion 115 electrolyte. Test conditions: cell temperature: 90°C, fully humidified DME anode and cathode, anode/cathode pressure: 1/1 atm, ξ_{DME}: 0.5 A/cm^2 equivalent (constant flow rate), ξ_c: 0.35 A/cm^2 equivalent (constant flow rate).

Figure 8. DME individual and overall electrode polarization curves with Nafion 117 electrolyte. Test conditions: cell temperature: 95°C, fully humidified DME anode and cathode, anode/cathode pressure: 3/1.7 atm, ξ_{DME}: 0.5 A/cm^2 equivalent (constant flow rate), ξ_c: 0.35 A/cm^2 equivalent (constant flow rate).

off region that is attributed to anode dryout. Note the polarization curves shown in Fig. 5 could not be extended beyond the maximum current density shown, because higher current densities resulted in unstable performance that decreased to zero cell voltage in time. Figure 6 shows a polarization curve taken for Nafion 115 with no such drop-off, suggesting this limitation is indeed due to anode dryout conditions. Figure 7 shows DMEFC polarization curve for Nafion 115 electrolyte under various operating pressures on the anode and cathode. Again, there was no sharp dropoff, indicating that the use of thinner electrolyte to promote back diffusion of water eliminated the anode dryout condition. However, a thinner electrolyte also permitted increased levels of DME crossover, which may have reacted parasitically at the cathode. From Fig. 7, the operating pressure made little change on the performance of the DMEFC except when there was a favorable pressure differential between the anode and cathode. In that case, some additional convective trans-
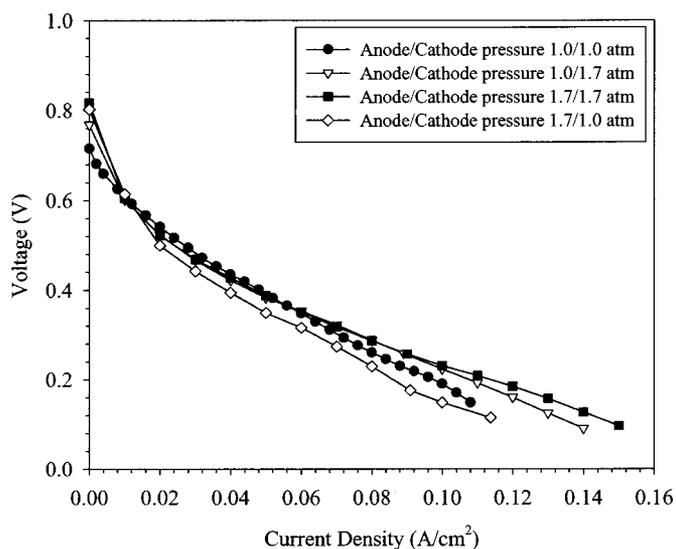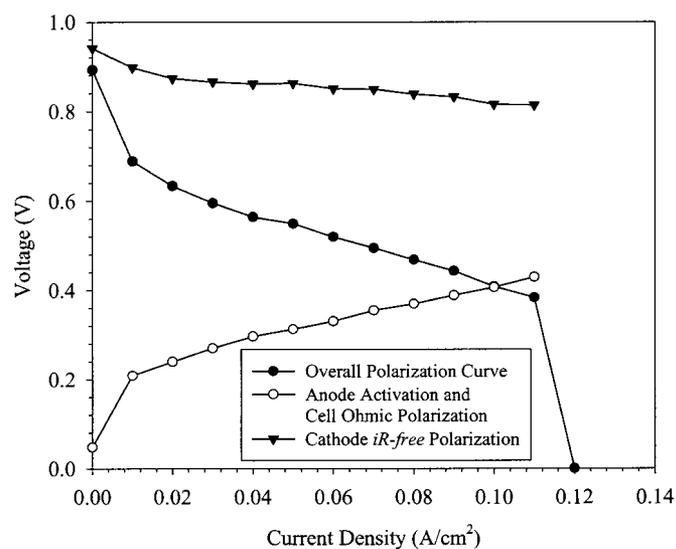
port of DME or water from anode to cathode may have resulted in increased ohmic or parasitic crossover reaction losses, respectively.

Performance results with Nafion 112 electrolyte.—Tests were conducted with Nafion 112 (51 µm thick) electrolyte. Various different test conditions of temperature, pressure, and humidity all resulted in no appreciable performance, for several different MEAs, no matter what preconditioning method was used. However, operation as an H$_2$ PEFC was at high performance levels, indicating no problems with the fuel cell, MEA, or data acquisition. For this series of tests, both hydrophobic and hydrophilic anode gas diffusion layers were used, with no change in results. This indicates that the DME crossover reaction may be concentration dependent. Note the open circuit voltage of the Nafion 117 and 115 were progressively lower, an indication of oxidation reaction of DME or DME intermediate crossover at the cathode. Note also that the anode mole fraction of DME was highly diluted due to the high humidity level needed for operation.

Individual electrode polarization.—In order to delineate between anode and cathode losses without a separate reference electrode, humidified hydrogen gas was used in the cathode after a polarization curve was recorded under the test operating conditions with DME anode and an air cathode. In this case, the hydrogen cathode became the dynamic hydrogen reference electrode.[35-37] Despite some potential errors associated with this indirect measurement technique, it is expected to provide a good idea of the polarization behavior of the individual electrodes. Because the hydrogen cathode is expected to have very small losses, on the order of 10-20 mV,[14] these can be neglected and the measured overpotential with a DME solution anode and a hydrogen cathode will be essentially the anode overpotential plus cell ohmic losses. Comparison with a overall cell polarization curve at similar conditions then provides the cathode iR-free polarization. Figures 8 and 9 show results from such a test for Nafion 117 and Nafion 115, respectively. The overall cell polarization curve, as well as the measured anode and ohmic and the deduced iR-free cathode polarization are shown. For Nafion 117, it can be seen that a majority of the measured overpotential results from anode activation and ohmic losses. This is expected, considering the anode dryout condition previously discussed. In contrast is Fig. 9, which shows results for a thinner Nafion 115 electrolyte. Here, the losses were dominated by iR-free cathodic activation overpotential.
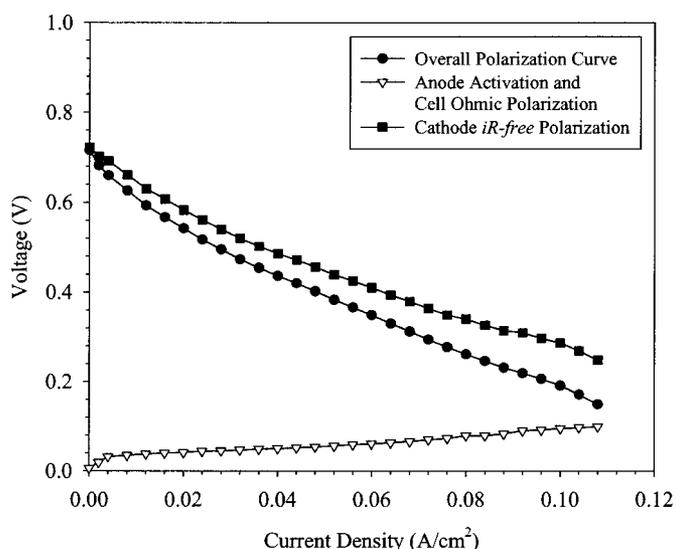

Figure 7. DME polarization curve with Nafion 115 electrolyte for various anode and cathode pressures. Test conditions: cell temperature: 90°C, fully humidified DME anode and cathode, ξ_{DME}: 0.5 A/cm^2 equivalent (constant flow rate), ξ_c: 0.35 A/cm^2 equivalent (constant flow rate).

Figure 9. DME individual and overall electrode polarization curves with Nafion 115 electrolyte. Test conditions: cell temperature: 90°C, fully humidified DME anode and cathode, anode/cathode pressure: 1.0/1.0 atm, ξ_{DME}: 0.5 A/cm² equivalent (constant flow rate), ξ_c: 0.35 A/cm² equivalent (constant flow rate).

This is another indication that (*i*) the anode dryout limitation was alleviated with the thinner electrolyte and (*ii*) there was some parasitic cathode DME or DME intermediate reaction. Figure 10 shows the anodic activation and fuel cell ohmic losses for a Nafion 115 electrolyte with methanol and DME for comparison. It can be seen that the anodic overpotential was quite similar under those conditions with a Pt-Ru anode. This encouraging result indicates that cathode catalyst optimization and crossover reduction is critical to ensure high performance of the DMEFC. The authors are currently conducting such a study.

Conclusions

The DMEFC offers many potential advantages compared to the conventionally used hydrogen or methanol for portable applications.
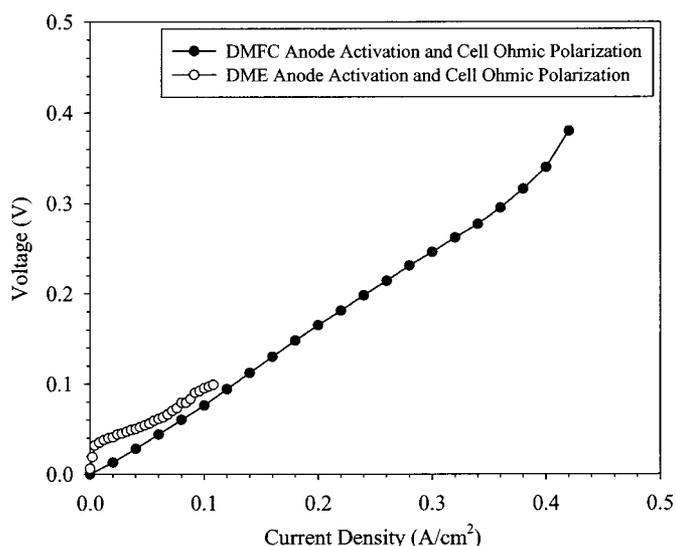

Figure 10. Activation plus ohmic polarization comparison between DMEFC and DMFC with Nafion 115 electrolyte. Test conditions: cell temperature: 90°C, fully humidified DME anode and cathode, anode/cathode pressure: 1.0/1.0 atm, ξ_{DME}: 0.5 A/cm² equivalent (constant flow rate), ξ_c: 0.35 A/cm² equivalent (constant flow rate).

While DMEFC stacks would presently be larger than equivalent DMFC stacks, the lack of fuel pump and low toxicity compared to methanol would reduce system size, weight, and complexity significantly. Equations were derived to show there is a critical balance between the requirement for anodic water content and DME mole fraction. Therefore, it is essential that thin electrolytes with high back diffusion are used. However, there appears to be a limit in electrolyte thickness below which DME crossover degrades performance to zero with a Pt cathode and Pt/Ru anode. An ongoing study is underway to determine an optimal anode and catalyst combination. Other conclusions from this study include:

1. Some aspect of surface CO adsorption may be necessary for adequate DMEFC performance. MEAs preconditioned in neat H_2 had very low relative performance, while those preconditioned by operation with methanol or CO-tainted hydrogen showed consistently measurable performance. That performance did not degrade over several hours time, indicating that the surface adsorbed CO species were not consumed without replacement during DME electro-oxidation.

2. With 178 μm Nafion 117 electrolyte, there was a sharp dropoff in performance due to anode dryout conditions. Use of a 127 μm Nafion 115 electrolyte to promote back diffusion of water to the anode eliminated this performance dropoff.

3. Use of a 51 μm Nafion 112 electrolyte was not possible due to reduction of performance to zero. This suggests that the crossover oxidation reaction of DME or DME intermediates is concentration dependent.

4. Electrode polarization data showed very different behavior depending on electrolyte thickness. For thicker Nafion 117, which was demonstrated to result in anode dryout conditions, the cell suffered high ohmic or anodic activation losses. For a thinner Nafion 115, the cathode displayed high relative performance loss and anodic polarization similar to a DMFC. This indicates that the DME or DME intermediate crossover is likely reacting parasitically at the cathode, and performance with thicker electrolytes was hindered by anode dryout.

Appendix

In this section, the derivation of Eq. 7 in the text is explained fully. The total reactant inlet molar concentration is calculated by the ideal gas law

$$c_{total} = \left| \frac{P}{RT} \right| \tag{A-1}$$

where P is gas channel inlet total pressure, R is universal gas constant, and T is cell temperature. DME molar concentration and inlet gas flow velocity are determined as follows

$$c_{DME} = (1 - X_{H_2O})_{in} c_{total} \tag{A-2}$$

$$\nu = \xi_{DME} \frac{i_{ref}}{12F} \frac{A_{Rx}}{A_x} \frac{RT}{\left(1 - RH \frac{P_{sat}}{P}\right)_{in} P} \tag{A-3}$$

where X is mole fraction of gas species at the anode gas channel inlet, P_{sat} is the saturation pressure corresponding to humidification temperature, and RH is the inlet relative humidity. The molar flow rates of DME and water vapor in can be shown as

$$\dot{n}_{\text{DME,in}} = c_{\text{DME}} \nu A_x = \xi_{\text{DME}} \frac{i_{\text{ref}} A_{\text{Rx}}}{12F} \qquad [\text{A-4}]$$

$$\dot{n}_{\text{H}_2\text{O,in}} = c_{\text{H}_2\text{O}} \nu A_x \qquad [\text{A-5}]$$

$$= \frac{RHP_{\text{sat}}}{RT} \xi_{\text{DME}} \frac{i_{\text{ref}} A_{\text{Rx}}}{12FA_x} \frac{RT}{\left(1 - RH\dfrac{P_{\text{sat}}}{P}\right)_{\text{in}} P} A_x \qquad [\text{A-6}]$$

$$= \frac{1}{(P/P_{\text{sat}}RH - 1)_{\text{in}}} \xi_{\text{DME}} \frac{i_{\text{ref}} A_{\text{Rx}}}{12F} \qquad [\text{A-7}]$$

Water is transported by electro-osmotic drag (from anode to cathode) and by concentration gradient driven back diffusion across the MEA. The net water transport rate through the MEA between anode and cathode is given by

$$\dot{n}_{\text{H}_2\text{O,tran}} = n_{\text{d}} \frac{i A_{\text{Rx}}}{F} - F_{\text{diff}} \qquad [\text{A-8}]$$

where $\dot{n}_{\text{H}_2\text{O,tran}}$ is the molar transport rate across the MEA, n_{d} is the electro-osmotic drag coefficient, i is the current density, and F_{diff} is the water transported by back diffusion. Assuming the amount of transported water by back diffusion is negligible (the most severe case for the anode to lose water and typical of thick membranes), Eq. A-8 can be simplified to

$$\dot{n}_{\text{H}_2\text{O,tran}} \leqslant n_{\text{d}} \frac{i A_{\text{Rx}}}{F} (\because F_{\text{diff}} \geqslant 0) \qquad [\text{A-9}]$$

The molar flow rate of DME at the anode gas channel outlet is given by

$$\dot{n}_{\text{DME,out}} = \dot{n}_{\text{DME,in}} - \dot{n}_{\text{DME,consumed}} - \dot{n}_{\text{DME,crossover}} \qquad [\text{A-10}]$$

$$= \xi_{\text{DME}} \frac{i_{\text{ref}} A_{\text{Rx}}}{12F} - \frac{i A_{\text{Rx}}}{2F} - \frac{i_{\text{crossover}} A_{\text{Rx}}}{12F} \qquad [\text{A-11}]$$

$$= \frac{(\xi_{\text{DME}} i_{\text{ref}} - i - i_{\text{crossover}})}{12F} A_{\text{Rx}} \qquad [\text{A-12}]$$

$$= \frac{(\xi_{\text{DME}} i_{\text{ref}} - i - 0.1)}{12F} A_{\text{Rx}} \qquad [\text{A-13}]$$

where i is the cell operating current density in A/cm^2, and we assume the equivalent crossover current density ($i_{\text{crossover}}$) is 100 mA/cm^2, based on research by Müller.[5] Similarly, the molar flow rate of water at the anode outlet can be calculated as follows

$$\dot{n}_{\text{H}_2\text{O,out}} = \dot{n}_{\text{H}_2\text{O,in}} - \dot{n}_{\text{H}_2\text{O,drag}} - \dot{n}_{\text{H}_2\text{O,consumed}} \qquad [\text{A-14}]$$

$$= \frac{1}{(P/P_{\text{sat}}RH - 1)_{\text{in}}} \xi_{\text{DME}} \frac{i_{\text{ref}} A_{\text{Rx}}}{12F} - n_{\text{d}} \frac{i A_{Rx}}{F} - \frac{i A_{\text{Rx}}}{4F} \qquad [\text{A-15}]$$

$$= \frac{A_{\text{Rx}}}{F} \left[\frac{\xi_{\text{DME}} i_{\text{ref}}}{12(P/P_{\text{sat}}RH - 1)_{\text{in}}} - n_{\text{d}} i - 0.25i \right] \qquad [\text{A-16}]$$

Thus, the mole fraction of water at the gas channel outlet is given by

$$X_{\text{H}_2\text{O,out}} = \frac{\dfrac{A_{\text{Rx}}}{F}\left[\dfrac{\xi_{\text{DME}} i_{\text{ref}}}{12(P/P_{\text{sat}}RH - 1)_{\text{in}}} - n_{\text{d}} i - 0.25i\right]}{\dfrac{A_{\text{Rx}}}{F}\left[\dfrac{\xi_{\text{DME}} i_{\text{ref}}}{12(P/P_{\text{sat}}RH - 1)_{\text{in}}} - n_{\text{d}} i - 0.25i\right] + \dfrac{(\xi_{\text{DME}} i_{\text{ref}} - i - 0.1\text{A/cm}^2)}{12F} A_{\text{Rx}}} \qquad [\text{A-17}]$$

If the anode outlet still contains water vapor, the numerator of Eq. A-17 should be greater than zero; that is

$$\frac{\xi_{\text{DME}} i_{\text{ref}}}{12(P/P_{\text{sat}}RH - 1)_{\text{in}}} - i(n_{\text{d}} + 0.25) \geqslant 0 \qquad [\text{A-18}]$$

which can be rearranged in the form of Eq. 7 in the text.

References

1. J. T. Wang, S. Wasmus, and R. F. Savinell, *J. Electrochem. Soc.,* **142**, 4218 (1995).
2. M. Weber, J. T. Wang, S. Wasmus, and R. F. Savinell, *J. Electrochem. Soc.,* **143**, L158 (1996).
3. S. R. Naranyanan, E. Vamos, S. Surampudi, H. Frank, G. K. Surya Prakash, M. C. Smart, R. Knieler, G. A. Olah, J. Kosek, and C. Cropley, *J. Electrochem. Soc.,* **144**, 4195 (1997).
4. J. T. Wang, W. F. Lin, M. Weber, S. Wasmus, and R. F. Savinell, *Electrochim. Acta,* **43**, 3821 (1998).
5. J. T. Müller, P. M. Urban, W. F. Hölderich, K. M. Colbow, J. Zhang, and D. P. Wilkinson, *J. Electrochem. Soc.,* **147**, 4058 (2000).
6. E. Peled, T. Duvdevani, A. Ahron, and A. Melman, *Electrochem. Solid-State Lett.,* **4**, A38 (2001).
7. F. Joensen and J. R. Rostrup-Nielsen, *J. Power Sources,* **105**, 195 (2002).
8. C. Lamy, A. Lima, V. LeRhun, F. Delime, C. Coutanceau, and J.-M. Léger, *J. Power Sources,* **105**, 283 (2002).
9. E. Peled, V. Livshits, and T. Duvdevani, *J. Power Sources,* **106**, 245 (2002).
10. Z. Qi and A. Kaufman, *J. Power Sources,* **110**, 65 (2002).
11. C. Rice, S. Ha, R. I. Masel, P. Waszczuk, A. Wieckowski, R. Barnard, *J. Power Sources,* **111**, 83 (2002).
12. Z. Qi, A. Kaufman, *J. Power Sources,* **112**, 121 (2002).
13. A. Oliveira Neto, M. J. Giz, J. Perez, E. A. Ticianelli, and E. R. Gonzalez, *J. Electrochem. Soc.,* **149**, A272 (2002).
14. S. Gottesfeld, in *Advances in Electrochemical Science and Engineering*, C. Tobias, Editor, p. 5, Wiley & Sons, New York (1997).
15. C. Lamy, J.-M. Léger, and S. Srinivasan, in *Modern Aspects of Electrochemistry*, J. O' M. Bockris and B. E. Conway Editors, p. 34, Plenum Press, New York (2000).
16. M. M. Mench, C. Y. Wang, and S. T. Thynell, *I. J. Trans. Phenomena,* **3**, 151 (2001).
17. D. Chu and S. Gilman, *J. Electrochem. Soc.,* **141**, 1770 (1994).
18. X. Ren, T. E. Springer, and S. Gottesfeld, *J. Electrochem. Soc.,* **147**, 92 (2000).
19. X. Ren, T. E. Springer, T. A. Zawodzinski, and S. Gottesfeld, *J. Electrochem. Soc.,* **147**, 466 (2000).
20. S. Thomas, X. Ren, S. Gottesfeld, and P. Zelenay, *Electrochim. Acta,* **47**, 3741 (2002).
21. L. Rubino and M. J. Thompson, Paper 993589, Society of Automotive Engineers Technical Publication (1999).
22. J. E. Sinor Consultants, Inc., *Dimethyl Ether as a Transportation Fuel: A-State-of-the-Art Survey*, U.S. Department of Energy (1997).
23. Material Safety Data Sheet, Dimethyl Ether, Praxair, form no. P-4589-B, (Oct 1997).
24. J. B. Hansen and B. Voss, Paper 950063, Society of Automotive Engineers Technical Publication (1995).
25. Y. Tsutsumi, S. Takasumi, and Y. Akihiro, in *Advanced Alcohol Fuel World, Proceedings of the 12th International Symposium on Alcohol Fuels*, p. 403 Tsingua University Press, Beijing, China (1998).
26. Y. Tsutsumi, T. Marakami, Y. Nakano, and S. Yamashita, in Abstracts of the 2002 Fuel Cell Seminar, p. 216, http://www.fuelcellseminar.com/index.asp (2002).
27. E. P. Murray, S. J. Harris, and H. Jen, *J. Electrochem. Soc.,* **149**, A1127 (2002).
28. S. Freni, M. Minutoli, N. Mondello, and S. Cavallaro, in Abstracts of the 2000 Fuel Cell Seminar, p. 704, http://www.fuelcellseminar.com/index.asp (2000).
29. G. J. Janssen, *J. Electrochem. Soc.,* **148**, A1313 (2001).
30. X. Ren, W. Henderson, and S. Gottesfeld, *J. Electrochem. Soc.,* **144**, L267 (1997).
31. X. Ren and S. Gottesfeld, *J. Electrochem. Soc.,* **148**, A87 (2001).
32. S. Ha, C. A. Rice, R. I. Masel, and A. Wieckowski, *J. Power Sources,* **112**, 655 (2002).
33. G. T. Burstein, C. J. Barnett, A. R. Kucernak, and K. R. Williams, *Catal. Today,* **38**, 425 (1997).
34. A. Hamnett, *Catal. Today,* **38**, 445 (1997).
35. T. I. Valdez and S. R. Narayanan, in *Proton Conducting Membrane Fuel Cells II*, S. Gottesfeld and T. F. Fuller, Editors, PV 98-27, p. 380, The Electrochemical Society Proceedings Series, Pennington, NJ (1998).
36. X. Ren, T. E. Springer, and S. Gottesfeld, *J. Electrochem. Soc.,* **147**, 92 (2000).
37. C. Lim and C. Y. Wang, *J. Power Sources,* **113**, 145 (2003).